Strain localization and cyclic damage of polyurethane foam cylinders: experimental tests and theoretical model

Giampiero Pampolini, Gianpietro del Piero

Strain localization and cyclic damage of polyurethane foam cylinders: experimental tests and theoretical model

Giampiero Pampolini [1,2], Gianpietro Del Piero [2]

[1] Laboratoire de Mécanique et d'Acoustique, CNRS, 31 chemin Joseph Aiguier, 13402 Marseille, France.
[2] Università di Ferrara, Via Saragat 1, 44100 Ferrara, Italy.

pampolini@lma.cnrs-mrs.fr; dlpgpt@unife.it

Abstract. Uniaxial compression tests performed by the authors on polyurethane foam cylinders show the typical stress-strain response curve of cellular materials, consisting of two ascending branches, separated by an almost horizontal plateau in which strain localization is observed. With less evidence, the same three regimes appear at unloading. Under cyclic deformation there is a progressive decay of the loading curve, while the unloading curve remains essentially the same at all cycles.
To describe this complex response we propose a rheological model, in which the foam is represented as a chain of nonlinear elastic springs with a non-convex strain energy, connected in parallel with a series of springs subject to progressive damage. The chain of springs models the strain localization, and the second series of springs reproduces the cyclic response. The overall stress-strain behavior of the model is in a good qualitative agreement with the experiments.

Keywords: polyurethane foams; strain localization; cyclic damage; non-convex strain energies; solid-solid phase change.

1 Introduction

We are interested in describing the mechanical behavior of polyurethane foam cylinders in uniaxial compression, with particular attention to two experimentally observed phenomena: strain localization, and the decay of the loading curve in a cyclic test.
Strain localization occurs with the formation of bands orthogonal to the direction of loading, see e.g. Gong et al. [7], Lakes et al. [8], and Pampolini and Del Piero [9]. This phenomenon is usually modeled by representing the foam as an assemblage of linear elastic beams, whose buckling determines the strain localization (Gibson and Ashby [6], Warren and Kraynik [12], Gong et al. [7]). In general, due to the complexity of the assumed microstructure, and to the difficulty of modeling the contact between beams in the post-buckling regime, this approach is very demanding from the computational point of

view [1]. An alternative approach is to consider the material as a hyperelastic continuum with non-convex strain energy density, and to use the non-convexity to model the band formation. This is the approach followed in [9], and briefly summarized here.
The decay of the loading curve in a cyclic compression test is shown in Figure 1, which also shows that the unloading curve is almost the same for all cycles. Though this behavior is reported in the literature, see e.g. Gong et al. [7], to our knowledge this phenomenon has never been modeled.
The cyclic behavior shown in Figure 1 has some analogy with the response of a rigid punch glued to a rigid plane by an adhesive layer with partially recoverable adhesion. For this type of response, a rheological model has been proposed in [4]. Here, this model is applied to polyurethane foams. To reproduce simultaneously cyclic damage and strain localization, this model is coupled with the strain localization model developed in [9]. The result is in a good qualitative agreement with the experimental response.

2 The experimental tests

In the compression tests performed at the *Laboratorio di Materiali Polimerici* of the University of Ferrara, ten specimens of a commercial polyurethane foam with dimensions $100 \times 100 \times 50$ mm were tested. For each specimen, four loading-unloading cycles were performed. A pre-load of 2 to 3 N was applied to assure an effective initial contact between plate and specimen. The crosshead speed, 5 mm/min in all tests, was sufficiently slow to render all rate-dependent effects negligible. A maximum displacement of 80% of the specimen thickness was sufficient to capture all significant aspects of the stress-strain curve. At unloading, to have a data acquisition without interruptions, it was necessary to stop the machine before re-attaining the initial configuration.
The loading curves in Figure 1 reveal the three-regime behavior characteristic of cellular materials: an initial almost linear response, followed by large displacements at almost constant load (plateau regime), and a final regime characterized by large stress increase under relatively moderate deformation. While at first loading the three regimes are evident, in the following cycles there is a smoother transition from the plateau to the second ascending branch. The loading curves decay as the number of cycles increases, but this decay stabilizes after five or four cycles [7]. The same occurs to the initial slopes of the loading curves. The three-regime behavior is less evident in the unloading curve which, as said above, is independent of the number of cycles.
The strain localization was detected following the deformation of a rectangular grid drawn on a side of the specimen. The progressive deformation of the grid is shown in Figure 2. As we see from Figure 2a, the deformation is initially homogeneous. Then a large deformation arises at the top of the specimen (Figure 2b), and propagates to the underlying layers (Figures 2c, 2d). After all layers have been reached, the specimen again deforms homogeneously (Figure 2e). The same deformation mechanism was observed by Wang and Cuitiño [11] in polyurethane low-density foams, and by Bastawros et al. [3] and Bart-Smith et al. [2] in aluminium alloy foams. That the large deformation starts at the upper end of the specimen can be attributed to local effects due to contact between steel plate

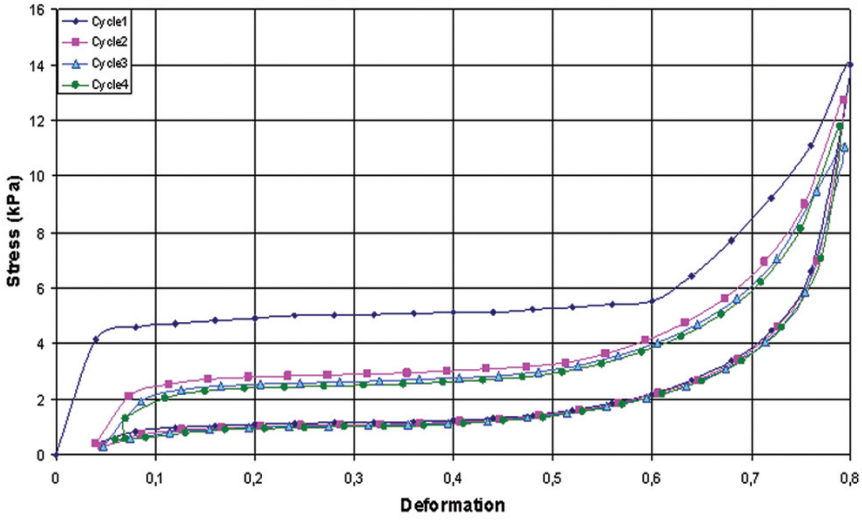

Figure 1: Experimental curves for polyurethane foams in a cyclic compression test [9].

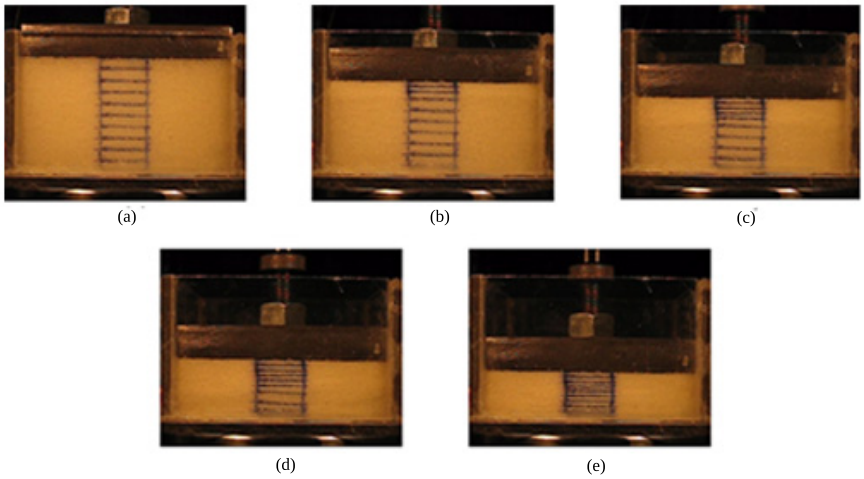

Figure 2: Progressive deformation mechanism. Initial homogeneous deformation (a). Strain localization at the upper end of the specimen (b). Propagation to the underlying layers (c), (d). Back to homogeneous deformation (e).

and the specimen's surface. In fact, in subsequent tests performed with different contact conditions, localization starts simultaneously at both sides.

3 The theoretical model

3.1 Strain localization

In this section we briefly describe the model for strain localization proposed in [9], in which the foam is represented as a chain of non-linear elastic springs with non-convex strain energy, and localization is attributed to progressive phase change. We suppose that the specimen be made of cells, as shown in Figure 3a, and that each layer of cells be represented by a non-linear elastic spring. The whole specimen is then represented by a chain of n springs, Figure 3b. We assume that all springs have the same non-convex energy $w = w(\varepsilon)$, where ε is the elongation of the spring.

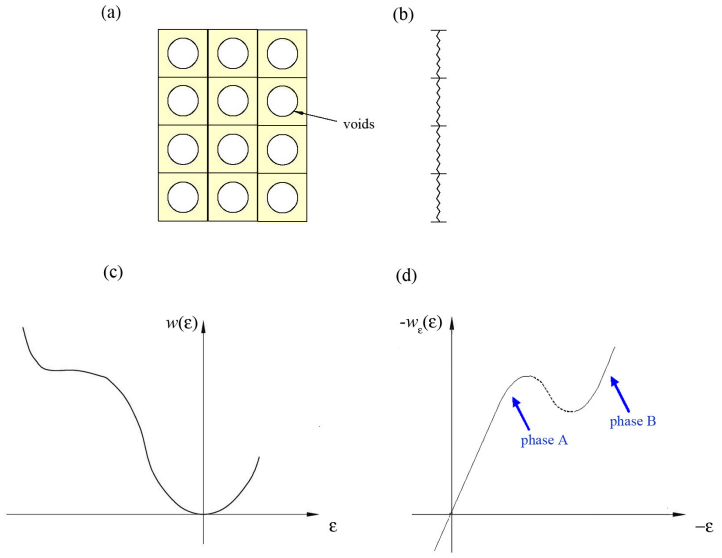

Figure 3: Subdivision of the body into cell layers (a), representation of each layer as a non linear elastic spring (b) with non convex energy (c), and non-monotonic stress-strain curve (d).

The form assumed for w is shown in Figure 3c. The corresponding stress-strain curve has two ascending branches separated by a descending branch, as shown in Figure 3d. The bar is subjected to the *hard device* condition

$$\sum_{i=1}^{n} \varepsilon_i = n\varepsilon_0, \tag{1}$$

where $n\varepsilon_0$ is the displacement of the upper basis, the displacement at the lower basis being zero.

The total energy of the chain is the sum of the energies of the springs. From the stationarity of the energy follows the equilibrium condition that the forces transmitted across the springs all have the same value σ. Moreover, if n is sufficiently large, a necessary condition for a local energy minimum is that all elongations ε_i lie on one of the two ascending branches of the stress-strain curve, see Puglisi and Truskinovsky [10] and Del Piero and Truskinovsky [5] for details. We say that the *i*-th spring is in the phase A if ε_i belongs to the first ascending branch, and that it is in the phase B if it belongs to the second ascending branch. Accordingly, any local energy minimizer has *m* springs in the phase A and $n - m$ springs in the phase B, with *m* between 0 and *n*. The local energy minimizers form metastable equilibrium paths in the configuration space. In Figure 4a, the projections of these paths in the (σ, ε_0) plane are shown for a chain made of four springs.

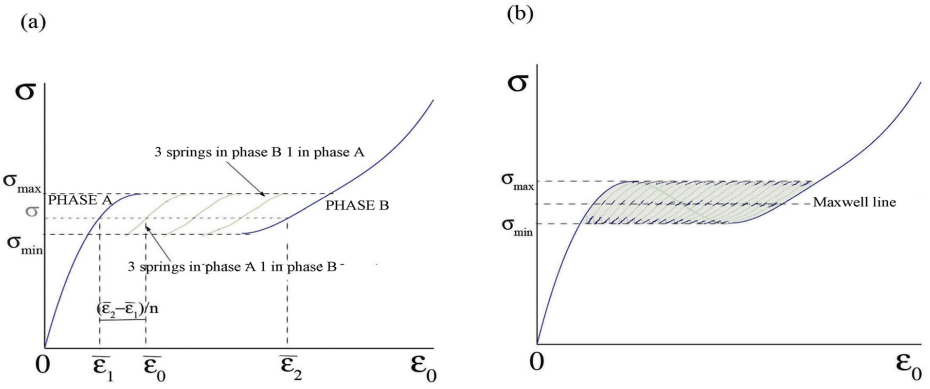

Figure 4: Response curves for a system of 4 springs (a) and for a system of 20 springs (b).

If one assumes that the system evolves along metastable equilibrium paths, then the system, when loaded starting from the initial configuration, initially follows the first ascending branch. This branch ends when σ reaches the value σ_{max} shown in Figure 4a. At this point, for further increasing deformation it is reasonable to assume that the system jumps to the closest stable branch, corresponding to the configuration with one spring in phase B and three springs in phase A. When this branch ends, the system jumps to the branch with two springs in phase B and so on, until all springs undergo the phase transition. At this point the system evolves following the second ascending branch, which corresponds to single-phase configurations with all springs in phase B.

If we now increase the number of the springs, the number of the intermediate branches increases, and the amplitudes of the jumps at the end of the branches decrease (Figure 4b). In this case, after the reaching of the critical value σ_{max} the system follows a wavy, approximately horizontal line. At unloading, the same behavior occurs after reaching the critical stress σ_{min}.

3.2 Cyclic damage

In this section we briefly describe the model for cyclic damage introduced by Del Piero [4]. The model applies to cellular foams, as well as to contact interfaces with partially recoverable adhesion; for simplicity, we first refer to the contact phenomenon.
Consider a rigid punch glued to a rigid plane. The glue is a linear elastic adhesive layer, in which the force σ transmitted across the layer is a function of the thickness u of the layer. When u attains a critical value u_0, a complete separation of the two rigid bodies occurs, and when the contact between punch and plane is re-established, the glue partially recovers its strength. More precisely, at each contact-separation cycle the elastic modulus of the layer is reduced with a prescribed law.
For a continuous process $t \mapsto u(t)$ with $u(0) = 0$, consider the sequences $n \mapsto t_n^-$ and $n \mapsto t_n^+$ defined as follows:

$$t_1^- = 0,$$

$$t_1^+ = \text{the smallest } t > 0 \text{ at which } u(t) = u_0,$$

$$t_n^- = \text{the smallest } t > t_{n-1}^+ \text{ at which } u(t) = 0,$$

$$t_n^+ = \text{the smallest } t > t_n^- \text{ at which } u(t) = u_0.$$

The half-open intervals $[t_n^-, t_n^+)$ and $[t_n^+, t_{n+1}^-)$ are the *n-th contact interval* and the *n-th separation interval*, respectively (Figure 5a). Note that the function $t \mapsto u(t)$ need not be monotonic in a contact or in an separation interval. We assume a constitutive relation of the form

$$\sigma = \begin{cases} A_n u & \text{in the n-th contact interval,} \\ 0 & \text{in all separation intervals,} \end{cases} \tag{2}$$

where A_n is a decreasing function of the number n of the cycles.
Let $t \mapsto u(t)$ be a cyclic process with maximum displacement $u_{max} > u_0$. In the first cycle, the response is linear, $\sigma = A_1 u$, for $u < u_0$, then drops to zero at $u = u_0$, and stays equal to zero at unloading (Figure 6a). In the the subsequent cycles the response is the same, except for the reduced slopes A_n of the loading lines.
Consider a system of four surface elements connected in parallel, with critical values u_{0i} satisfying

$$u_{01} < u_{02} < u_{03} < u_{04}\,,$$

and assume that the system is subjected to the cyclic process shown in Figure 5b, with amplitude u_{max} such that

$$u_{02} < u_{max} < u_{03}\,.$$

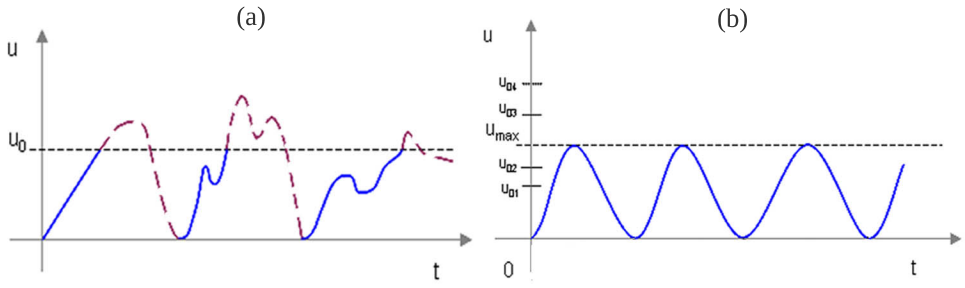

Figure 5: (a) Contact (full lines) and separation (dotted lines) intervals of a cyclic load process. (b) The cyclic load process with fixed maximum displacement.

Then at the n-th loading cycle the number of the contact-separation cycles is n for the first two elements, and zero for the last two.
The response curves of the system are shown in Figure 6b. Denote by A_{nk} the elastic modulus of the k-th element in the n-th contact interval. Initially, the response of the system is linear, with slope given by the sum of the moduli A_{1k}. At the reaching of the lowest critical value u_{01}, the first element moves to the separation regime, and its elastic modulus drops to zero. The same happens to the second element when the second critical value u_{02} is attained. In the rest of the first loading cycle and during the following unloading cycle, the system follows the line with slope $A_{13} + A_{14}$, represented by the dotted line in Figure 6b. In the subsequent loading cycles one has the same behavior, with the only difference that at the n-th cycle the moduli of the first two elements reduce to A_{n1}, A_{n2}, respectively. In conclusion, the total force acting on the system is

$$\sigma = \begin{cases} (A_{n1} + A_{n2} + A_{13} + A_{14})u & \text{for } u < u_{01} \text{ in the n-th loading cycle,} \\ (A_{n2} + A_{13} + A_{14})\, u & \text{for } u_{01} \le u < u_{02} \text{ in the n-th loading cycle,} \\ (A_{13} + A_{14})\, u & \text{for } u_{02} \le u \text{ in all loading cycles,} \\ (A_{13} + A_{14})\, u & \text{for all } u \text{ in all unloading cycles.} \end{cases} \tag{3}$$

For a large number of elements, the critical points $(u_{0k}, A_{1k}u_{0k})$ can be approximated by a continuous curve $\sigma = f(u)$, and the system's response can be approximated by the diagram shown in Figure 6c, see Del Piero [4] for details.
In the case of polyurethane foams, the specimen is again supposed to be formed of cells, as in Figure 3a. Each column of cells is now represented as a spring, and the springs are supposed not to interact with the neighboring ones. Each spring has a force-elongation relation of the type (5), with different elastic moduli A_{nk} and different critical values u_{0k} for each spring. In the following subsection, this model for cyclic damage is coupled with the previous model for strain localization.

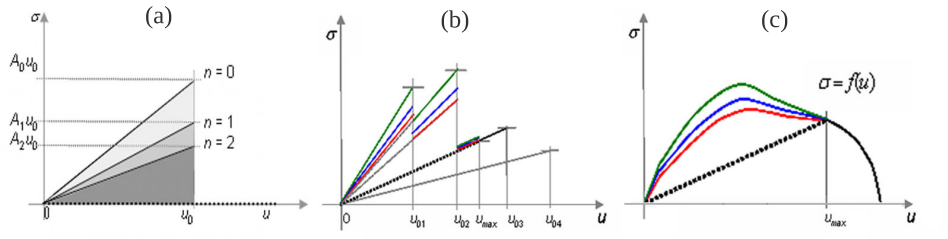

Figure 6: Response curves of a surface element undergoing contact with recoverable adhesion (a), of and of a system of four (b) and of a large number (c) of surface elements connected in parallel, subjected to the cyclic load process shown in Figure 5b.

3.3 The coupled model

Consider a system composed of a chain of M non-linear elastic springs of the type described in Subsection 3.1, connected in parallel with a series of N bulk elements of the type described in Subsection 3.2, as shown in Figure 7. We assume that both M and N are sufficiently large to consider as continuous the response curves of the springs and of the

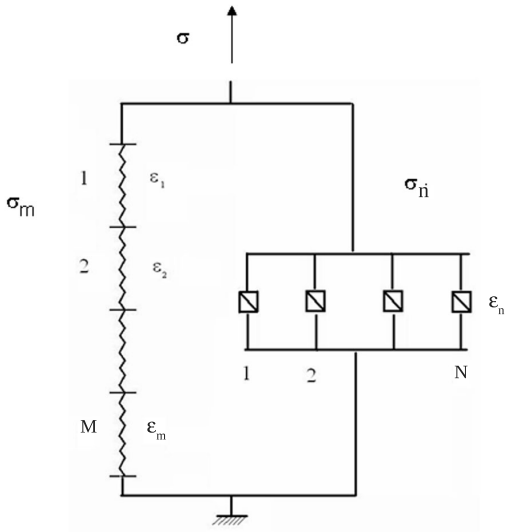

Figure 7: The coupled model. A chain of non linear elastic springs with non-convex strain energy connected in parallel with a series surface elements undergoing contact with recoverable adhesion.

bulk elements. In particular, we assume that the critical points $(u_{0i}, A_{1i}u_{0i})$ of the bulk elements approximate the curve with a horizontal asymptote shown in Figure 8b.

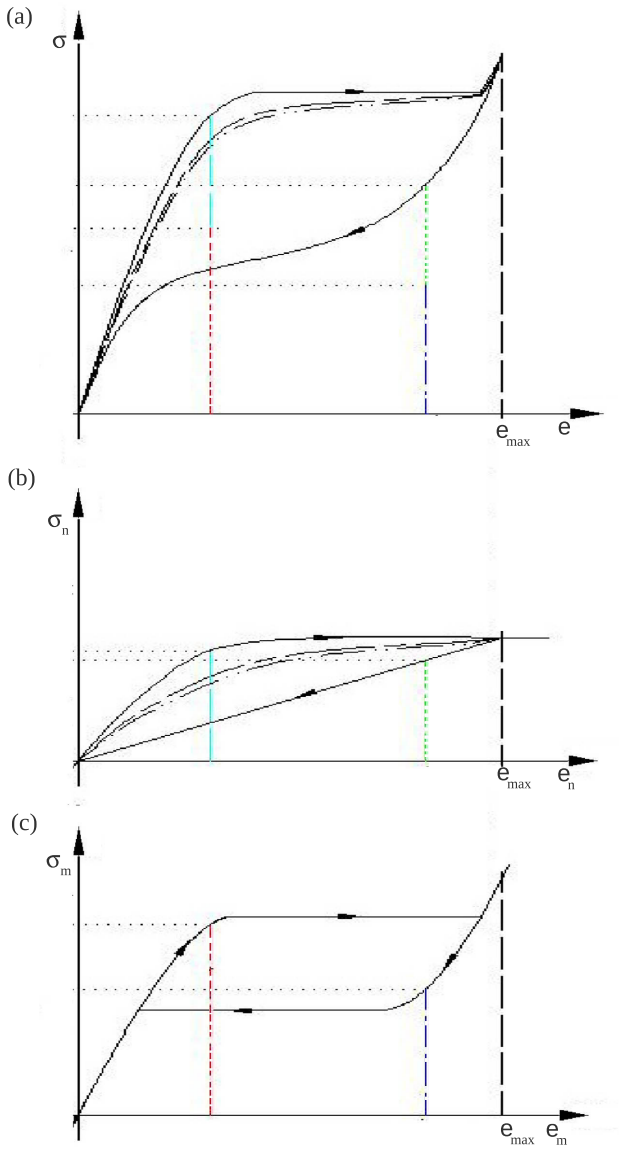

Figure 8: Construction of the response curves for the coupled model (a), as sums of the contributions of the cyclic damage (b) and of the strain localization (c) models.

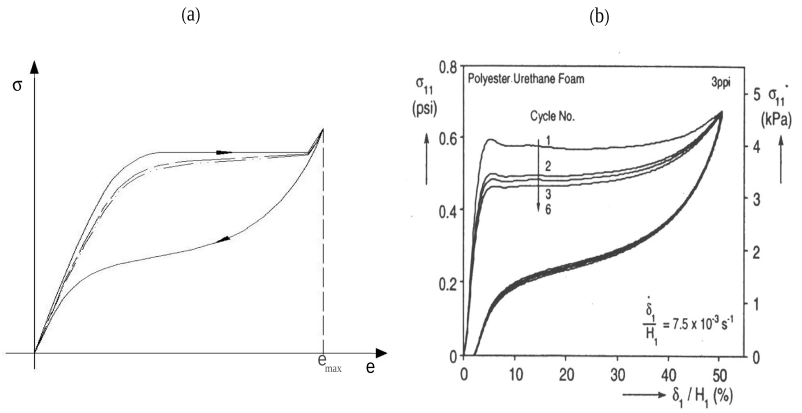

Figure 9: Comparison between the response curve of the coupled model in cyclic compression (a), and the experimental curves obtained by Gong et al. 2005 (b).

The total force σ is the sum of the total force σ_m in the springs and of the force σ_n in the bulk elements, with

$$\sigma_m = w'(\varepsilon_{mi})\,, \qquad i = 1, 2, ..., M\,, \tag{4}$$

$$\sigma_n = \sum_{k=1}^{N} A_{n_k k} \varepsilon_n\,, \tag{5}$$

where ε_{mi} are the elongations of the springs in the first system, ε_n is the elongation of each of the bulk elements in the second system, and

$$\varepsilon_n = \sum_{i=1}^{N} \varepsilon_{mi}\,. \tag{6}$$

The response curve for the coupled model can be constructed by adding up the response curves of the two systems, as shown in Figure 8. In Figure 9, the resulting curve is compared with the experimental curve given in [7]. We see a good qualitative agreement, both in the general features of the cyclic response and in the shape of the unloading curve.

References

[1] S. G. Bardenhagen, A. D. Brydon, and J. E. Guilkey. Insight into the physics of foam densification via numerical simulation. *J. Mech. Phys. Solids*, 53:597–617, 2005.

[2] H. Bart-Smith, A.-F. Bastawros, D. R. Mumm, A. G. Evans, D. J. Sypeck, and H. N. G. Wadley. Compressive deformation and yielding mechanisms in cellular

Al alloys determined using X-ray tomography and surface strain mapping. *Acta Materialia*, 46:3583–3592, 1998.

[3] A.-F. Bastawros, H. Bart-Smith, and A. G. Evans. Experimental analysis of deformation mechanisms in a closed-cell aluminium alloy foam. *J. Mech. Phys. Solids*, 48:301–322, 2000.

[4] G. Del Piero. A rheological model for cyclic damage and recoverable adhesion. *Forthcoming*, 2007.

[5] G. Del Piero and L. Truskinowsky. Elastic bars with decohesions. *Forthcoming*.

[6] L. J. Gibson and M. F. Ashby. *Cellular Solids: Structure and Properties*. Cambridge University Press, 2nd edition, 1997.

[7] L. Gong, S. Kyriakides, and W. Y. Jang. Compressive response of open-cell foams. part I: Morphology and elastic properties. *Int. J. Solids Struct.*, 42:1355–1379, 2005.

[8] R. Lakes, P. Rosakis, and A. Ruina. Microbuckling instability in elastomeric cellular solids. *J. Mater. Sci.*, 28:4667–4672, 1993.

[9] G. Pampolini and G. Del Piero. Strain localization in polyurethane foams. experiments and theoretical model. *Forthcoming*.

[10] G. Puglisi and L. Truskinovsky. Mechanics of a discrete chain with bi-stable elements. *J. Mech. Phys. Solids*, 48:1–27, 2000.

[11] Y. Wang and Y. Cuitiño. Full-field measurements of heterogeneous deformation patterns on polymeric foams using digital image correlation. *Int. J. Solids Struct.*, 39:3777–3796, 2002.

[12] W. E. Warren and A. M. Kraynik. Linear elastic behavior of a low-density kelvin foam with open cells. *ASME J. Appl. Mech.*, 64:787–793, 1997.